Properties of Periodic Gas Lenses

By D. MARCUSE

(Manuscript received June 18, 1965)

Gas lenses are being considered as focusing elements of beam-waveguides. Since very many lenses are needed to form a long waveguide, it is reasonable to consider periodic arrangements of gas lenses. Such periodic structures might operate with a gas stream which flows through all of the lenses in succession. A periodic temperature distribution in the gas results which is different from that of single gas lenses considered in two earlier papers.[3,4]

This paper analyses the ray optics properties, such as focal length and principal surfaces of the gas lenses, of two types of alternating gradient focusing systems. One system consists simply of a succession of hot and cold tubes. The other system results from the first by insertion of heat insulating tubes of equal length between the hot and cold tubes.

I. INTRODUCTION

The beam-waveguide described by Goubau[1] appears as a promising device to transmit light over long distances. However, to reduce the power loss due to absorption and reflection, which is inevitable with lenses made of solid dielectrics, gas lenses have been proposed[2,3] instead of the solid lenses used by Goubau.

Two earlier papers[3,4] discussed the properties of a particular type of gas lens. This tubular gas lens consists of a warm tube into which a cooler gas is blown. The thermal gradients in the gas lead to density gradients which give the structure the properties of a positive lens.

Ref. 4 discusses the focal length and principal surface of this gas lens for the case that the gas enters the lens at a constant temperature. It was shown that this device, when operated under optimum conditions, acted as an optically rather thin lens with moderate lens distortions.

The present paper extends the earlier analysis in several ways. We consider periodic lens structures. Such a structure results if hot and cold tubes are alternated to form a long, periodic structure. The gas is heated and cooled periodically giving rise to periodically arranged positive and negative lenses. A periodic structure of this type represents an alter-

nating gradient focusing system.[5] In general, the temperature of the gas entering the hot or cold tubes will not be constant over the cross section of the tube so that the earlier results are no longer applicable. The gas temperature in the periodic structure will also be periodic and will depend on the temperatures of the hot and cold tubes as well as on the flow velocity.

It is our aim to compute the temperature distribution in such periodic structures and use it to determine the properties of the equivalent lenses which describe the ray optics of the alternating gradient focusing systems.

The equivalent lenses are rather complicated. They are neither optically thin nor free of distortions. Further investigations are required to determine the guidance properties of an alternating gradient focusing system with imperfect lenses of this type.

We discuss two types of periodic gas lens systems. In one case we assume that hot and cold tubes of equal length are directly adjacent to each other. The other type is an alternating gradient beam-waveguide which consists of hot and cold tubes which are separated by tube sections made of an ideally heat insulating material. For simplicity it is assumed that the insulating sections are as long as the hot and cold tubes. The assumption of a perfectly heat insulating material is an overidealization since hardly any material conducts heat more poorly than gases. It is intended as an approximation to the real situation of imperfect heat insulators.

In the insulating tube sections, the gas has a chance to equalize its temperature. As it does so rather rapidly, we again have the case of hot and cold tubes being fed by an input gas at a constant temperature. However, the insulating sections act also as lenses in the same sense as the hot or cold tubes by which they are preceeded. Therefore, it is not surprising that some improvement of efficiency results if heat insulating tube sections are used to separate the hot and cold tubes. But this advantage is not very striking; and, since this analysis assumes ideally insulating tubes, it is not certain how much of a real advantage can be gained by using this construction. Considerably more experience is needed before a decision can be made.

This analysis again neglects all convection effects in the gas lenses.

To be able to distinguish which of the two structures is being discussed we will call the structure using hot and cold tubes without heat insulating tube sections the *simple periodic structure* while the second case which includes insulating sections will be called the *extended periodic structure*.

II. RAY TRACING

Before entering into a discussion of the simple and extended periodic structures, the ray tracing technique used to determine the focal length and principal surface of the lenses will be explained.

The trajectory of the light ray in the gas lens is given by the ray equation[6]

$$\frac{d}{ds}\left(n\frac{d\mathbf{r}}{ds}\right) = \text{grad } n \tag{1}$$

$\mathbf{r}$ = the position vector leading from an arbitrary origin to points on the ray.
n = index of refraction.
s = length coordinate measured along the ray.

We limit ourselves to rays which are very nearly parallel to the axis of the structure which is used as the z-coordinate so that we can replace s by z.* Assuming angular symmetry it is sufficient to consider the vector component in radial direction r perpendicular to the z-axis. Finally, we neglect the term

$$(\partial n/\partial z)\ (dr/dz)$$

because $dr/dz \ll 1$ for rays which are nearly parallel to the z-axis and also because the variation of n in the z-direction will generally be smaller than that in the r-direction.

$$(\partial n/\partial z) \ll (\partial n/\partial r).$$

With these assumptions we obtain from (1)

$$\frac{d^2r}{dz^2} = \frac{1}{n}\frac{\partial n}{\partial r}. \tag{2}$$

However, since we are only interested in gases where $n - 1 \ll 1$ we can safely write

$$\frac{d^2r}{dz^2} = \frac{\partial n}{\partial r}. \tag{3}$$

The index of refraction depends on temperature in the following way:

$$n - 1 = (n_0 - 1)\frac{T_0}{T} \tag{4}$$

T_0 is the absolute temperature at which n_0 is measured while T is the

* The error caused by this approximation is estimated in Ref. 4.

absolute temperature for which we want to determine n. It follows from (4) that

$$\frac{\partial n}{\partial r} = -(n_0 - 1)\frac{T_0}{T^2}\frac{\partial T}{\partial r}.$$

The value of the absolute temperature varies only slightly throughout the gas so that T can be replaced by a suitable average temperature. It is convenient to choose T_0 equal to this average temperature which should be chosen as

$$T_0 = \tfrac{1}{2}(T_h + T_c) \tag{5}$$

T_h = temperature of hot tubes
T_c = temperature of cold tubes

This leads us to the ray equation

$$\frac{d^2r}{dz^2} = -\frac{n_0 - 1}{T_0}\frac{\partial T}{\partial r}. \tag{6}$$

Equation (6) is our starting point for the ray optics of the gas lenses. Since $\partial T/\partial r$ is a complicated function of r and z, it is difficult to solve (6) analytically so that we content ourselves with numerical solutions obtained by means of an electronic computer.

Rather than expressing our results as functions of z, we want to obtain them as functions of the *on*-axis gas velocity v_0 normalized by a suitable constant V. (This representation was also used in Refs. 3 and 4.) We define $V(L)$ by

$$v_0/V(L) = a/\sigma L \tag{7}$$

with

$$\sigma = k/av_0\rho c_p \tag{8}$$

a = tube radius
L = tube length
k = heat conductivity of the gas
ρ = (average) gas density
c_p = specific heat at constant gas pressure.

Equation (7) shows that $v_0/V(L)$ is inversely proportional to the length of the tube. Therefore, it is convenient to introduce a variable

$$u(z) = a/\sigma z \tag{9}$$

which at $z = L$ equals

$$W = u(L) = \frac{v_0}{V(L)}. \tag{10}$$

Using

$$x = r/a \tag{11}$$

equation (6) becomes

$$\frac{d^2x}{du^2} + \frac{2}{u}\frac{dx}{du} = -\frac{1}{u^4}\frac{n_0 - 1}{\sigma^2 T_0}\frac{\partial T}{\partial x}. \tag{12}$$

Equation (12) is used to obtain x and dx/du as a function of W from which the focal length f and principal surface p can be computed.

As shown in Fig. 1(a), we follow the ray from a point $z = z_1$ to $z = z_2$, corresponding to $u = u_1$ and $u = u_2$, through the tube anticipating the case of lenses which are not bounded by planes through the ends of the tube but by surfaces inside of the tube to be defined later.

The definition of focal length and principal surface can be seen from Fig. 1(a). The principal surface is obtained by following a ray, which is incident parallel to the axis ($dx/dz = 0$ at $z = z_1$), through the lens. If we extend the direction of the ray entering the lens and the direction of the ray leaving the lens at $z = z_2$ by straight lines back into the lens we obtain a cross-over point which defines a point on the principal surface. The distance p of this point measured from the beginning of the tube as a function of x_1, the input position of the ray, describes the principal surface. The distance p_+ for rays traveling in the same direction as the gas flow is given by (Fig. 1(a))

$$p_+ = z_1 + L - \frac{x(z_2) - x(z_1)}{\left(\frac{dx}{dz}\right)_{z=z_2}} \tag{13}$$

or, expressed in terms of u and W rather than L

$$\frac{p_+}{L} = \frac{z_1}{L} + 1 + \frac{x(u_2) - x(u_1)}{u_2^2\left(\frac{dx}{du}\right)_{u=u_2}} W. \tag{14}$$

We define the focal length as the distance from the intersection of the incoming ray (extended in a straight line) with the principal surface to the point at which the outgoing ray crosses the axis of the structure.

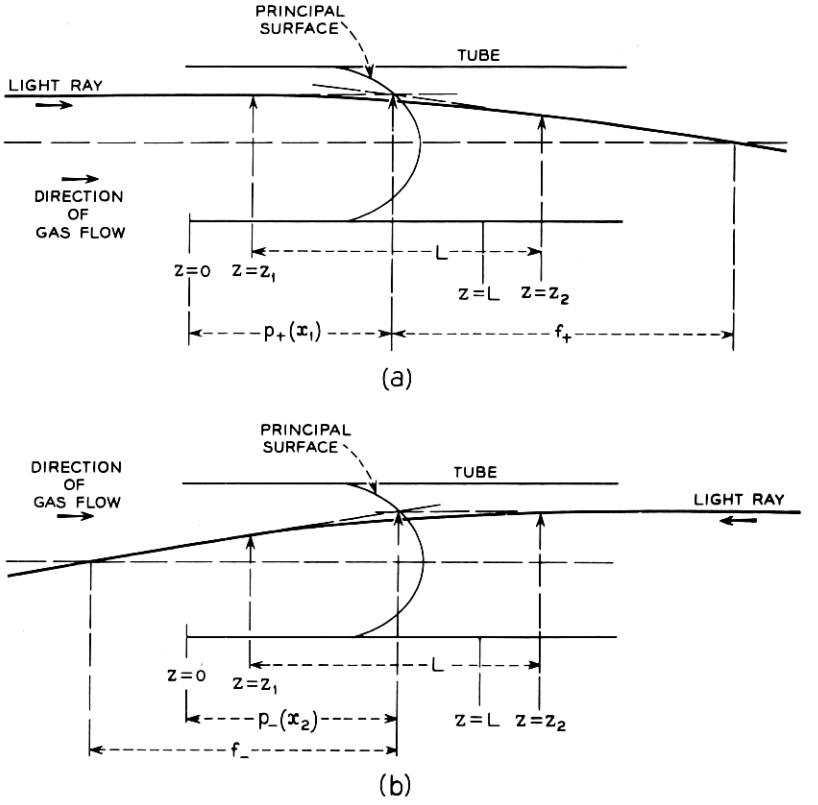

Fig. 1 — Geometry of a single gas lens showing the definition of focal length and principal surfaces.

Therefore, we have

$$f_+ = -\frac{x(z_1)}{\left(\frac{dx}{dz}\right)_{z=z_2}} \tag{15}$$

or, in terms of u and W,

$$\frac{f_+}{L} = W\frac{x(u_1)}{u_2^2\left(\frac{dx}{du}\right)_{u=u_2}}. \tag{16}$$

Similarly, we obtain from Fig. 1(b) the principal surface and focal

length for the ray traveling in opposite direction to the gas flow

$$\frac{p_-}{L} = \frac{z_1}{L} - W \frac{x(u_2) - x(u_1)}{u_1^2 \left(\frac{dx}{du}\right)_{u=u_1}} \tag{17}$$

and

$$\frac{f_-}{L} = -W \frac{x(u_2)}{u_1^2 \left(\frac{dx}{du}\right)_{u=u_1}} . \tag{18}$$

The principal surfaces p_+ and p_- do not, in general, coincide. If they are identical the lens is called optically thin. The separation between the two principal surfaces is an indication of the optical thickness of the lens.

III. THE SIMPLE PERIODIC STRUCTURE

3.1 *Temperature Distribution*

The simple periodic structure consists of alternating hot and cold tubes (Fig. 2). In order to compute the equivalent positive and negative lenses of this structure we first have to determine the temperature distribution.

The temperature distribution is given by a series expansion[7] which, in the hot tube, reads

$$T_1(x,u) = T_h - \sum_{n=0}^{\infty} A_n R_n(x) \exp\left(-\beta_n^2/u\right) \tag{19}$$

$$\infty > u > W = \frac{v_0}{V(L)}$$

with T_h being the wall temperature of the hot tube and $u = a/\sigma z$; and

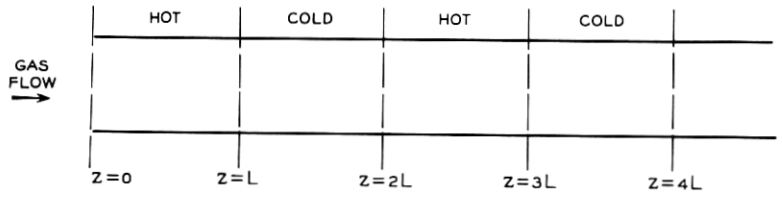

Fig. 2 — Sequence of hot and cold tubes comprising the "simple periodic structure".

in the cold tube

$$T_2(x,u) = T_c - \sum_{n=0}^{\infty} B_n R_n(x) \exp\left\{-\beta_n^2 \cdot \left(\frac{1}{u} - \frac{1}{W}\right)\right\} \tag{20}$$

with

$$W > u > \tfrac{1}{2}W$$

T_c = wall temperature of cold tube
$W = a/\sigma L$.

The functions R_n and the eigenvalues β_n are discussed in the appendix. The coefficients A_n and B_n have to be determined so that the temperature is a periodic function in the simple periodic structure of Fig. 2.

To simplify the determination of A_n and B_n we limit ourselves to sufficiently long tubes or slow enough flow velocities so that the first term of the series expansions (19) and (20) are sufficient to describe the temperature distribution at the end of each tube accurately. This condition is expressed by the requirements

$$W = \frac{v_0}{V(L)} < 10. \tag{21}$$

The periodicity condition requires that the temperature at the end of the cold tube ($z = 2L$ or $u = \frac{1}{2}W$) equals the temperature at the beginning of the hot tube ($z = 0$ or $u = \infty$)

$$T_1(x,\infty) = T_2(x,\tfrac{1}{2}W). \tag{22}$$

In addition, we have to require that the gas temperature passes continuously from the hot to the cold tube

$$T_1(x,W) = T_2(x,W). \tag{23}$$

The conditions (21) to (23) allow the determination of the constants A_n and B_n

$$A_n = -\frac{2(T_h - T_c)}{\beta_n \left(\frac{\partial R_n}{\partial \beta}\right)_{x=1}} \left\{1 - \frac{\delta_{on}}{1 + \exp\left(\beta_0^2 \frac{1}{W}\right)}\right\} \tag{24}$$

and

$$B_n = -A_n \tag{25}$$

with

$$\delta_{on} = \begin{cases} 1 & n = 0 \\ 0 & n \neq 0. \end{cases}$$

The eigenvalues β_n and the derivation $\partial R/\partial \beta$ are given in the appendix.

The temperature distribution in the hot tube is shown in Fig. 3(a) for $v_0/V(L) = 5$ and in Fig. 3(b) for $v_0/V(L) = 10$ as a function of normalized radium $x = r/a$. The various curves in each figure correspond to different positions along the tube axis. At $z = 0$ the temperature distribution is identical to that at the end of the cold tube. The temperature is cold on the wall and warmer in the center of the tube. As we follow the temperature distribution deeper into the hot tube we see that the temperature on the wall changes instantly from its value equal to the wall temperature of the cold tube to that of the hot tube. However, the slope of the temperature distribution close to the tube axis remains negative for quite some length. This means that the gas in the hot tube acts like a negative lens close to the input end of the tube. It takes some distance to reverse the negative temperature gradient which the cold tube imparted to the gas. In fact, there exists a neutral surface in the hot as well as the cold tube which is defined by the points where the temperature gradient $\partial T/\partial x = 0$. On this surface the gas acts neither as a positive nor negative lens. The neutral surface separates the region

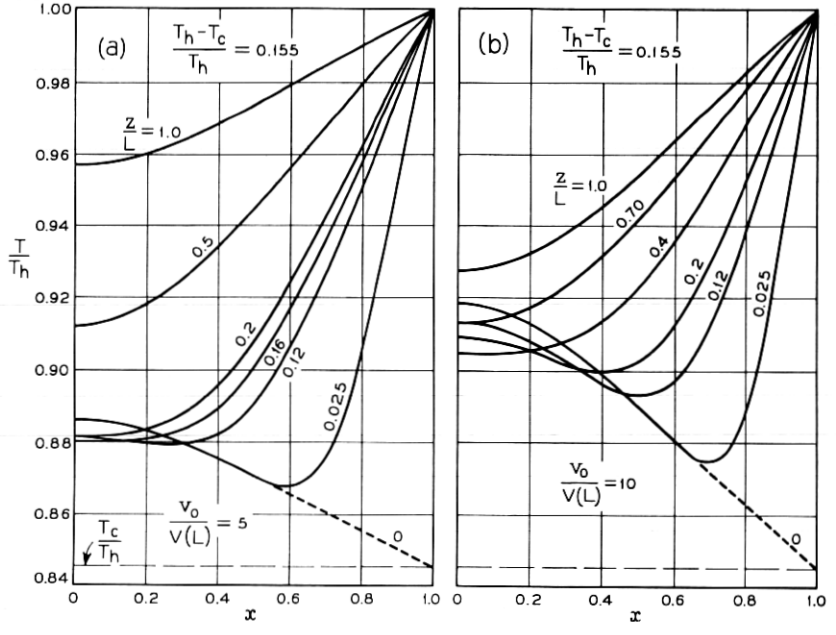

Fig. 3(a) — Temperature distribution in the simple periodic structure as a function of normalized radius $x = r/a$ at various cross sections z/L in the tube. The normalized flow velocity is $v_0/V(L) = 5$ and $(T_h - T_r)/T_h = 0.155$.

Fig. 3(*b*) — Same as Fig. 3(a) with $v_0/V(L) = 10$.

of the positive from the negative lens. It has the same shape in the hot as well as the cold tube and the distance between corresponding points of these surfaces in either tube is L, the length of the hot and cold tubes. The temperature distribution T/T_h in the cold tube is obtained by reflecting each point of the temperature distribution of Fig. 3(a) or 3(b) on the line parallel to the x-axis at $T/T_h = T_h + T_c/2T_h$. The neutral surfaces, z/L as a function of x, for various values of flow velocity are obtained by rotating the curves of Fig. 4 around the z-axis. At high gas velocities ($v_0/V(L) = 10$) the neutral surface extends almost to the half way point into the hot and cold tubes.

3.2 *Focal Length and Principal Surface*

To calculate effective lenses which describe the ray optics properties of the hot and cold tubes it is not permissible to trace rays through each tube and compute focal length data from the ray trajectory since each tube functions as a combination of positive and negative lenses. It is more reasonable to trace rays from one neutral surface to the next since the gas between two neutral surfaces acts entirely in one sense either as a positive or negative lens.

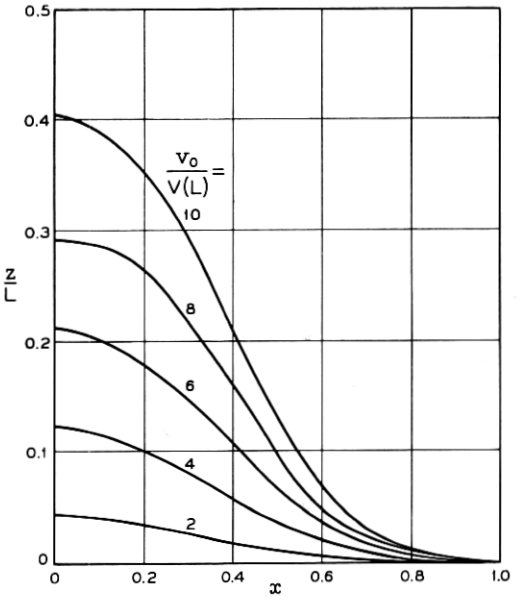

Fig. 4 — Shape of the neutral surfaces for various values of $v_0/V(L)$.

We inject a ray at a point z_1 , $x(z_1)$ on the neutral surface with a slope $(dx/dz)_{z=z_1} = 0$ and follow it to the point $z_2 = z_1 + L$, $x(z_2)$. This point does not, in general, lie on the next neutral surface since the ray moves from its entrance position, $x(z_1) \neq x(z_2)$. However, this point z_2 , $x(z_2)$ lies sufficiently close to points on the next neutral surface that this ray tracing procedure seems justified.

Our present discussion explains the meaning of the points z_1 and z_2 (or correspondingly u_1 and u_2) introduced in (13) through (18) and shown in Fig. 1.

The slope and positions of rays entering at $z = z_1$ with $dx/dz = 0$ were computed at $z = z_2$ by numerical integration of (12). The temperature distribution entering into (12) is given by (19) and (20). The values of the slope and the ray position were then used to calculate the focal length and principal surface from (14) and (16). The rays traveling in the direction opposite to the gas flow were launched at $z = z_2$, $x(z_2)$ on the neutral surface with the slope $(dx/dz)_{z=z_2} = 0$ and their slope and position at $z_1 = z_2 - L$, $x(z_1)$ was used to calculate p_-/L and f_-/L from (17) and (18).

It is apparent from (12) and (24) that all of our results depend on a parameter

$$D = \frac{n_0 - 1}{\sigma^2} \frac{T_h - T_c}{T_0} . \tag{26}$$

However, we like to plot our results as functions of $W = v_0/V(L)$ which is contained in σ. It is therefore convenient to write

$$D = \left(\frac{v_0}{V(L)}\right)^2 C\left(\frac{L}{a}\right) \tag{27}$$

and use

$$C\left(\frac{L}{a}\right) = (n_0 - 1) \frac{T_h - T_c}{T_0} \left(\frac{L}{a}\right)^2 \tag{28}$$

to characterize the focusing power of the lens.* Fig. 5 shows the focal length f divided by the length L of the tubes as a function $v_0/V(L)$. The solid curves represent the positive, the broken curves the negative lens. The focal length of the negative lens is shown as a positive quantity. These curves were computed setting $x(z_1) = 0.1$. The positive and negative lenses have almost equal focusing power for small values of $C(L/a)$. The negative lens has more focusing power for larger values

* In reference 4 $C(L/a)$ was defined slightly differently. There, $T_h - T_c$ was replaced by $T_h - T_i$ (T_i temperature of input gas).

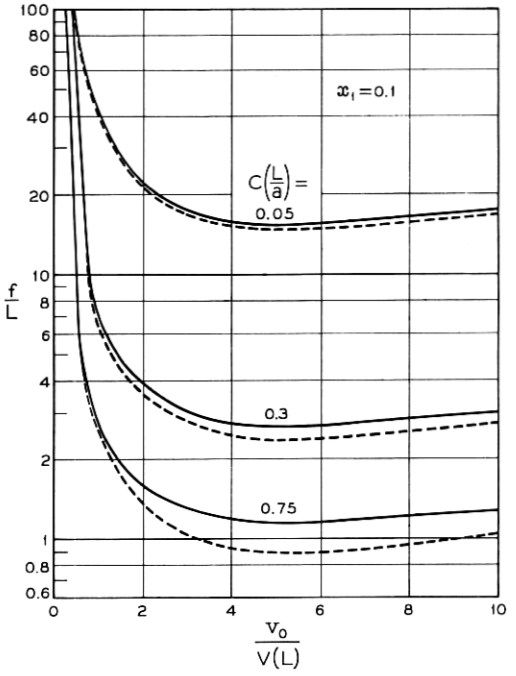

Fig. 5 — Normalized focal length f/L of the positive (solid lines) and negative (broken lines) lenses of the simple periodic structure as functions of the normalized flow velocity $v_0/V(L)$.

of this parameter. The temperature gradients are equal but opposite in sign for either of these lenses so that one might expect that they should have equal focusing power. The discrepancy is explained by considering that the rays travel through different parts of the lenses. In the positive lens the ray starting at $x(z_1) = 0.1$ moves closer towards the lens axis while the ray in the negative lens, starting at the same point, moves away from the axis and toward the wall.

The minima of the focal length curves are explained by the fact that we have no lens action if the gas is stationary, $v_0/V(L) = 0$. The lens begins to function with increasing gas flow. But, if the gas finally flows so fast that the *on*-axis temperature does not have time to follow, lens action ceases again. Interpolation of curves for parameter values other than those shown in Fig. 5 is facilitated by noting that the focal length is nearly proportional to $[C(L/a)]^{-1}$.

The focal length of an ideal lens does not depend on the input position $x(z_1)$ of the ray. Plotting f/L as a function of x should result in a straight

line parallel to the x-axis. That gas lenses are not ideal lenses is shown in Figs. 6(a) through 6(e). These figures contain three different types of curves. The solid curves represent the positive lens for rays traveling in the same direction as the gas while the dotted curves represent rays traveling opposite to the gas flow. The dash-dotted curves give the results for the negative lens and rays in the positive gas direction. The rays opposite to the gas flow in the negative lens have been ommitted. They can be visualized by the fact that the curves in the two directions coincide at $x = 0$. At $x = 0.9$ the curves for the negative lens join up with the dotted lines of the positive lens. The lines for the negative lens do not all extend to $x = 0.9$ because the ray in the negative lens moves toward the wall and may hit it before it travels its full length if the lens is too strong and if the ray started out sufficiently close to the wall.

Figs. 6(a) through 6(e) show that there are focal length distortions for smaller values of $v_0/V(L)$. For $v_0/V(L) = 6$ and 8 the focal length curves are substantially parallel to the x-axis. (We see, furthermore, that the focal length for the two directions of propagation coincide more closely for smaller values of $C(L/a)$ and x.

The principal surfaces are shown in Figs. 7(a) through 7(e). The meaning of the solid, dotted and dash-dotted curves is the same as explained above. The dash-dotted lines for the negative lens for the low values of $C(L/a)$ coincided very nearly with the solid line for the positive lens and was omitted. Also not shown are the corresponding curves for the negative lens for rays traveling against the gas flow. The principal surfaces are far from being plane. It is also apparent that for most values of $C(L/a)$ and x, the two principal surfaces for the two directions of the beams don't coincide too closely. This shows not only that the lenses comprising the simple periodic structure have considerable distortions but also that they are not optically thin under all conditions.

Fig. 8 shows the dependence of the point $x = 0.1$ of the principal surfaces on the flow velocity $v_0/V(L)$. The principal surfaces move to $z = 0$ for vanishing flow velocities and extend far into the tube for large values of $v_0/V(L)$.

IV. THE EXTENDED PERIODIC STRUCTURE

4.1 *Temperature Distribution*

The extended periodic structure is shown in Fig. 9. It consists of alternating positive and negative lenses which are separated by pieces of insulating tubes of equal length.

The temperature distribution, T_3, in the hot or cold tubes is well

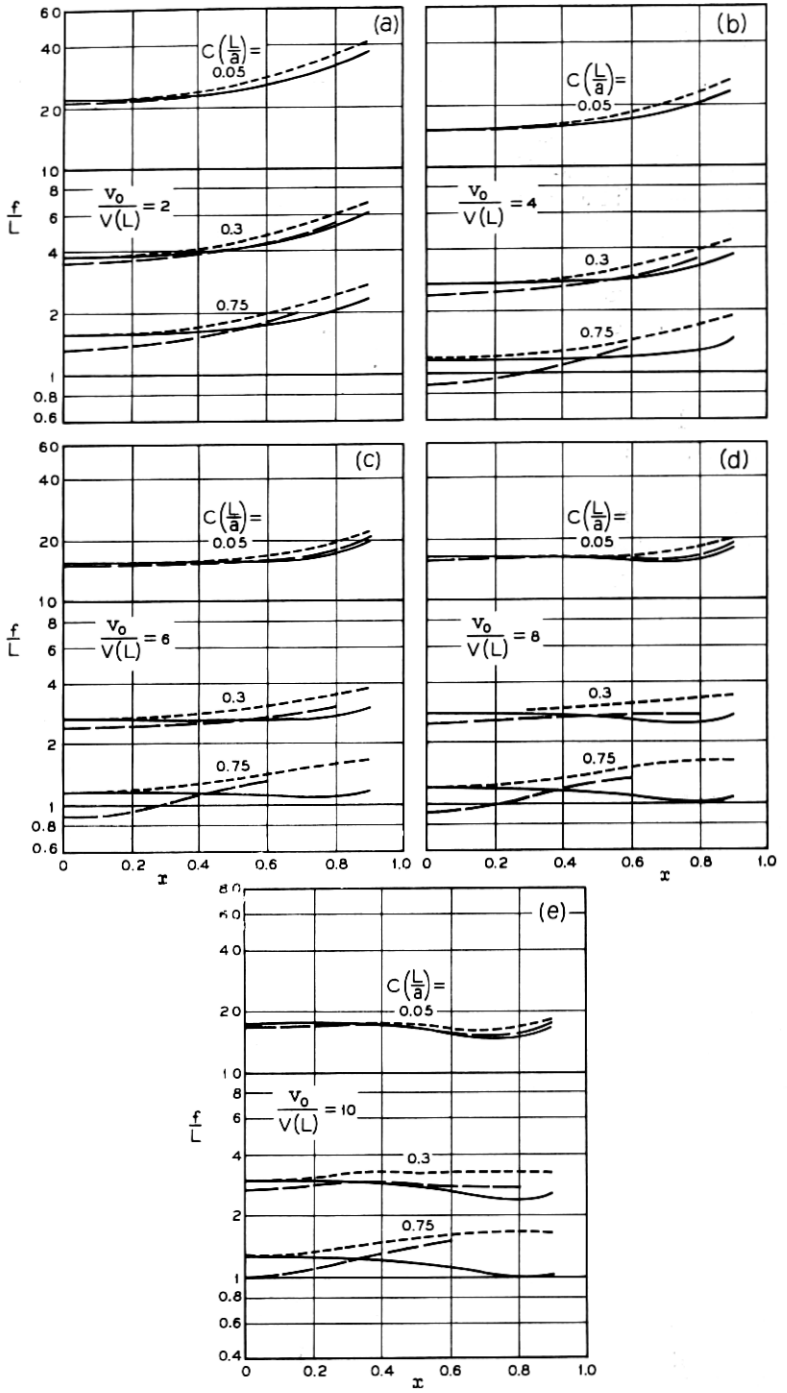

Fig. 6 — Normalized focal length f/L as a function of the ray's position $x = r/a$ for rays in the positive lens traveling (1.) with the gas stream (solid lines), and (2.) against the gas stream (dotted lines); and for rays in the negative lens traveling with the gas stream (dash-dotted lines).

known[3,7] if we can assume that the input gas is at a constant temperature.

$$T_3(x,u) = T_W + 2(T_W - T_i) \sum_{n=0}^{\infty} \frac{R_n(x)}{\beta_n \left(\frac{\partial R_n}{\partial \beta}\right)_{\substack{x=1 \\ \beta=\beta_n}}} \exp\left(-\beta_n^2/u\right) \qquad (29)$$

$$\infty > u > W$$

T_W = either T_h, temperature of hot tube, or T_c, temperature of cold tube.
T_i = input temperature to the hot or cold tubes.
W = $v_0/V(L)$ with L length of hot or cold tubes.

The temperature distribution, T_4, in the insulating sections is given in terms of U-functions and their eigenvalues γ which are defined in the appendix.

$$T_4(x,z) = A_0 + \sum_{n=1}^{\infty} A_n U_n(x) \exp\left[-\gamma_n^2 \left(\frac{1}{u} - \frac{1}{W}\right)\right] \qquad (30)$$

$$W > u > \tfrac{1}{2}W.$$

The expansion coefficients have to be determined from the condition

$$T_3(x,W) = T_4(x,W). \qquad (31)$$

Since the exponential functions appearing in (29) and (30) decrease very rapidly with decreasing values of u, it is sufficient to consider only the first term in the expansion at the end of each tube. This is justified if

$$0 \leqq W < 10. \qquad (32)$$

Condition (31) leads to

$$A_0 = T_W - 8(T_W - T_i) \frac{R_0'(1) \exp\left(-\beta_0^2/W\right)}{\beta_0^3 \left(\frac{\partial R_0}{\partial \beta}\right)_{\substack{x=1 \\ \beta=\beta_0}}} \qquad (33a)$$

and for $n \neq 0$

$$A_n = -4(T_W - T_i) \frac{\gamma_n R_0'(1) \exp\left(-\beta_0^2/W\right)}{\beta_0(\gamma_n^2 - \beta_0^2) \left(\frac{\partial R_0}{\partial \beta_0} \cdot \frac{\partial U'}{\partial \gamma_n}\right)_{x=1}} \qquad (33b)$$

where we have used the notation $F' = dF/dx$.

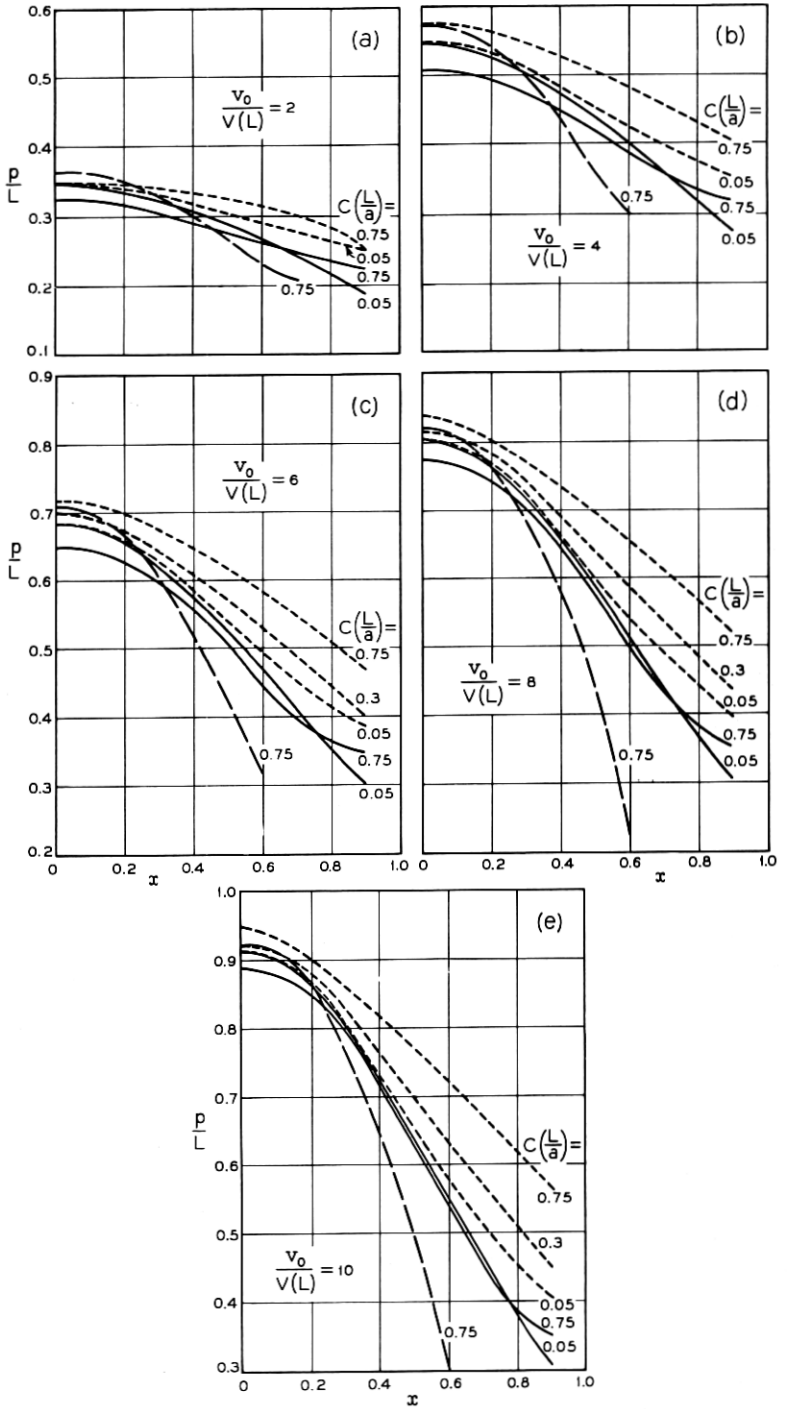

Fig. 7 — The principal surface for rays in the positive lens traveling (1.) with the gas stream (solid lines), and (2.) against the gas stream (dotted lines); and for rays in the negative lens traveling with the gas stream (dash-dotted lines).

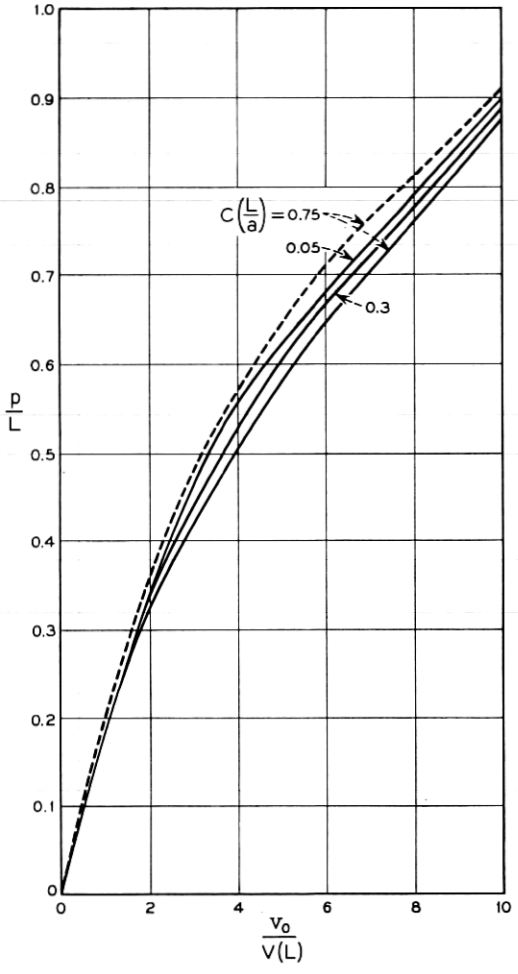

Fig. 8 — The dependence of the point of the principal surface at $x = 0.1$ on the gas velocity. The solid lines represent the positive lens, the dash-dotted lines the negative lens for rays traveling with the gas stream.

The temperature distribution in the hot and cold tubes can be inferred from curves shown in Ref. 3. The temperature distribution in the insulating tubes is shown in Fig. 10(a) for $\sigma(L/a) = 0.15$ ($W = 6.67$) and in Fig. 10(b) for $\sigma(L/a) = 0.05$ ($W = 20$) for various values of $\sigma[(z - L)/a]$. $z - L$ is the length coordinate counting from the beginning of the insulating tube. The curves show the temperature as a function of radius at different distances from the input to the insulating

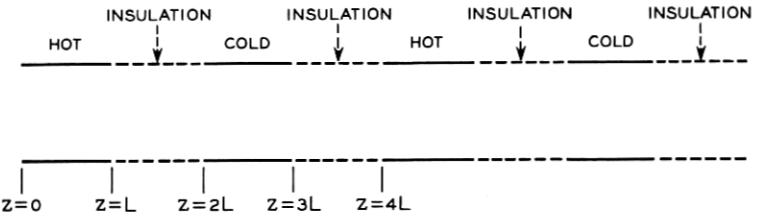

Fig. 9 — The hot, cold and insulating tubes comprising the "extended periodic structure".

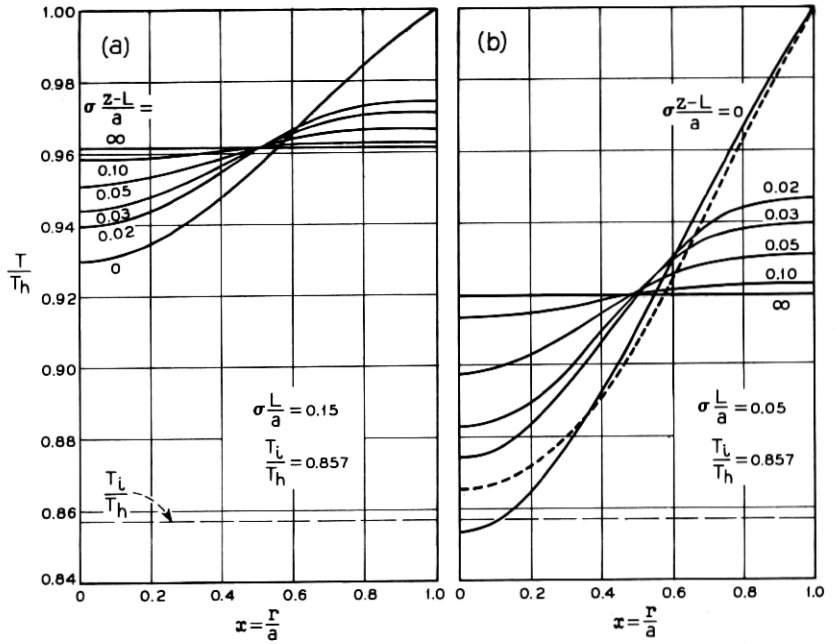

Fig. 10(*a*) — Temperature distribution in the insulating tubes of the extended periodic structure following a hot tube. $\sigma[(z - L)/a]$ is the normalized length measured from the beginning of the insulating tube. The ratio of input temperature to the preceeding hot tube T_i over its wall temperature T_h is $T_i/T_h = 0.857$. The normalized length of the tubes is $\sigma L/a = 0.15$.

Fig. 10(*b*) — Same as Fig. 10(*a*). $\sigma L/a = 0.05$. The dotted line is the actual temperature distribution at the end of the hot tube while the line with $\sigma\,[\,(z - L)/a] = 0$ is the temperature distribution at the end of the hot tube which results from dropping all but the first term in the series expansion of (29).

tube. At $z - L = 0$, the temperature distribution is identical to that at the output end of the hot tube feeding the insulating tube. It is apparent that the temperature equalizes rather rapidly. For practical purposes we can say that the temperature has reached a constant value at $\sigma[(z - L)/a] \geqq 0.1$. If we consider insulating tubes of length L, equal to the length of the hot or cold tubes feeding them, we obtain constant output temperatures of the insulating tubes for values $0 \leqq W < 10$. The hot and cold tubes are fed by gas at a constant temperature as long as these conditions are met. Therefore, we are justified in using (29) which has been derived for the case that the gas at the input end of the tube is at a constant temperature.

In the periodic structure of Fig. 9, the input temperature T to the hot and cold tubes are not arbitrary. They adjust themself to satisfy the periodicity condition

$$(T_3(x,u))_{z=0} = (T_4(x,u))_{z=4L}. \tag{34}$$

With the help of (34) we can calculate the input temperature T_{ih} of the hot or T_{ic} of the cold tube from (29), (30) and (33).

We obtain from (30) and (33a), for the constant output temperature of the insulating tube following the hot tube, ($W < 10$ is assumed so that all exponential terms $\exp(-\gamma_n^2/W)$ can be neglected)

$$(T_4(x))_{z=2L} = T_{ic} = T_h - 8(T_h - T_{ih}) \frac{R_0'(1) \exp(-\beta_0^2/W)}{\beta_0^3 \left(\frac{\partial R_0}{\partial \beta}\right)_{\substack{x=1 \\ \beta=\beta_0}}}$$

and also

$$(T_4(x))_{z=4L} = T_{ih} = T_c - 8(T_c - T_{ic}) \frac{R_0'(1) \exp(-\beta_0^2/W)}{\beta_0^3 \left(\frac{\partial R_0}{\partial \beta}\right)_{\substack{x=1 \\ \beta=\beta_0}}}.$$

Here we have two equations which allow us to determine the two quantities T_{ih} and T_{ic}.

It is convenient to express them in the form

$$\frac{T_h - T_{ih}}{T_h - T_c} = \left\{1 + 8 \frac{R_0'(1) \exp(-\beta_0^2/W)}{\beta_0^3 \left(\frac{\partial R}{\partial \beta}\right)_{\substack{x=1 \\ \beta=\beta_0}}}\right\}^{-1} \tag{35a}$$

and

$$\frac{T_{ic} - T_c}{T_h - T_c} = \frac{T_h - T_{ih}}{T_h - T_c}. \tag{35b}$$

A plot of (35a) as a function of $W = v_0/V(L)$ is shown in Fig. 11.

4.2 *Focal Length and Principal Surface*

The following graphical representations show the focal length and principal surface of one hot and insulating or one cold and insulating tube. The extended periodic structure is thus transformed into a system of equivalent positive and negative lenses in the same way as in the case of the simple periodic structure. Fig. 12 shows the dependence of the normalized focal length f/L on the normalized flow velocity $v_0/V(L)$ for a ray entering at $r/a = 0.1$. The length L is that of the hot tube and not the total length of the combination of hot and insulating tubes which has the length $2L$. The solid curve in Fig. 12 shows the focal length of the combination of hot and insulating tubes while the dotted curve shows the focal length of the hot tube alone for comparison. It is obvious that the insulating tube adds to the focusing power of the gas lens. We terminated the curves at $v_0/V(L) = 10$ since we wanted to remain in the domain of (32) where our simplifying assumptions used to calculate the temperature distribution are valid. Fig. 13 shows the corresponding

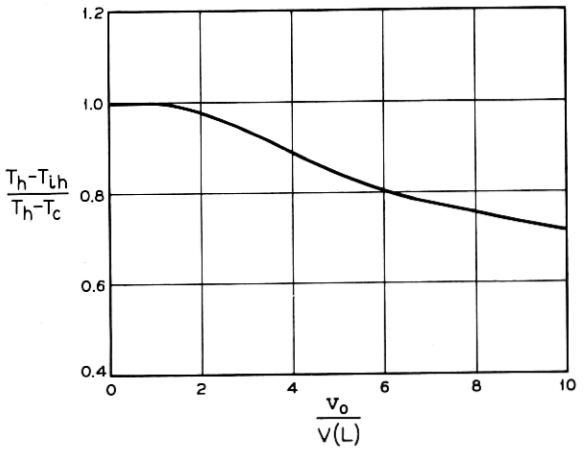

Fig. 11 — Temperature difference between the hot tube T_h and the input temperature to the hot tube T_{ih} divided by the temperature difference $T_h - T_c$ between hot and cold tube as a function of normalized gas velocity $v_0/V(L)$.

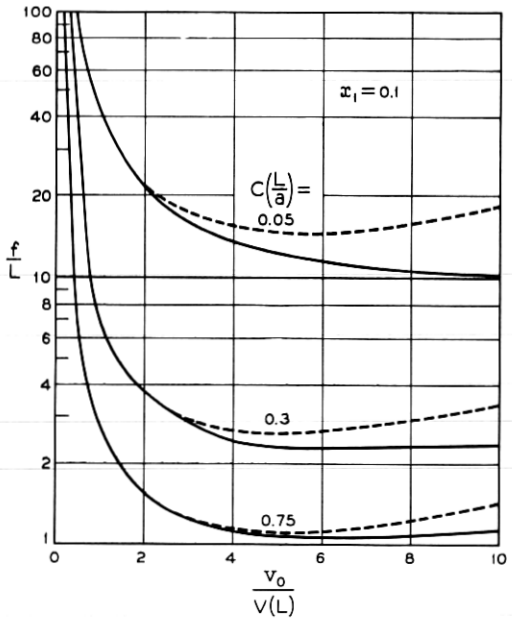

Fig. 12 — Normalized focal length f/L of the positive lenses of the extended periodic structure (solid lines) and of the hot tubes alone (dotted lines) as functions of normalized flow velocity $v_0/V(L)$.

curves for the cold tube resulting in a negative lens. A comparison of the two figures shows that the negative lens is more powerful than the positive lens for corresponding values of $C(L/a)$.

Figs. 14(a) and (b) show the dependence of the focal length (measured from the principal surface) on the input position, $x = r/a$, of the ray for the hot plus insulating tubes. The solid lines represent rays traveling in the same direction as the gas while the dotted curves show the focal length of rays traveling in opposite direction to the gas flow.

The shape of the principal surfaces for the hot plus insulating tube are shown in Fig. 15(a) and (b). The distance p of points on the principal surface is measured from the gas input end of hot tube. The solid and dotted lines again represent rays traveling with and against the gas flow respectively. The principal surface is far from being a plane for larger values of $v_0/V(L)$. The two principal surfaces do not coincide exactly which means that the lens has some optical thickness for larger values of $C(L/a)$.

The corresponding negative lens shows very similar distortions and has therefore been omitted.

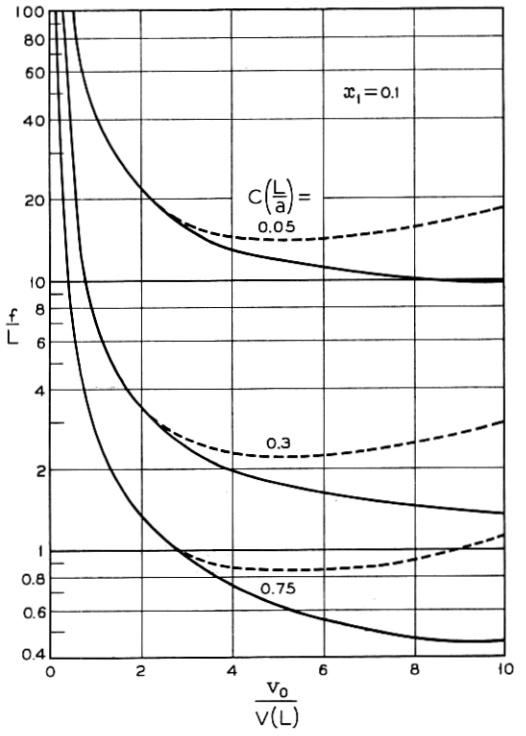

Fig. 13 — Normalized focal length f/L of the negative lenses of the extended periodic structure (solid lines) and of the cold tubes alone (dotted lines) as functions of the normalized flow velocity $v_0/V(L)$.

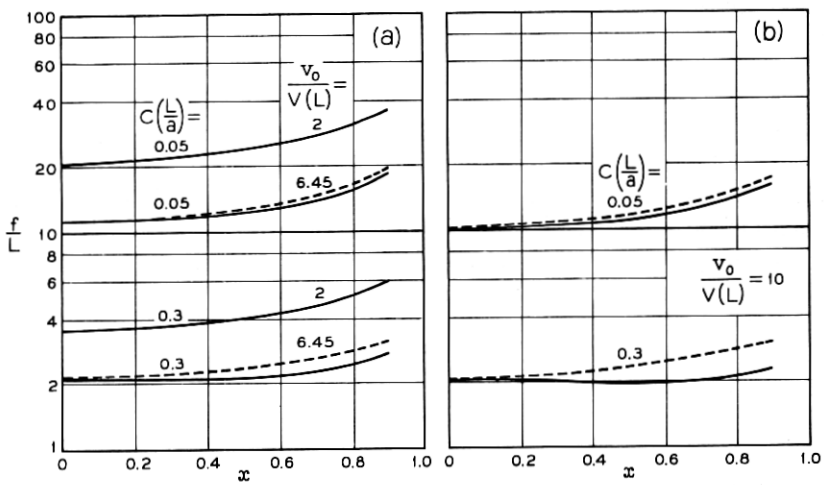

Fig. 14 — Dependence of focal length on the ray's input position for the positive lenses of the extended periodic structure for rays traveling with the gas flow (solid lines) and against the gas flow (dotted lines).

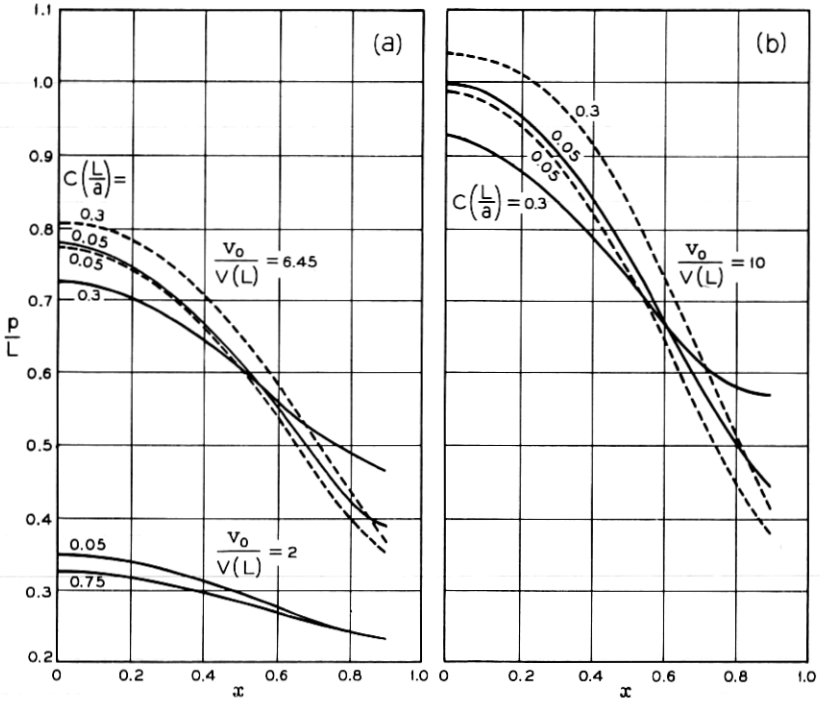

Fig. 15 — The principal surface of the positive lenses of the extended periodic structure for rays traveling with the gas flow (solid lines) and against the gas flow dotted lines.

V. COMPARISON OF THE TWO PERIODIC STRUCTURES

In order to compare the two periodic structures let us assume that their equivalent lenses are spaced at the same distance D. For the simple periodic structure D, the distance between a positive and the next negative lens is equal to the length L of the individual tubes. In the extended periodic structure $D = 2L$. It seems fair to compare both structures under the condition that the actual gas velocities in either one of them are identical. However, this assumption requires some rescaling of the data of the extended structure. If we operate the simple structure at a certain value of $v_0/V(D)$ the corresponding value for the extended structure will be different since v_0 is the same but in the extended structure $D = 2L$. It is apparent that

$$\left(\frac{v_0}{V(L)}\right)_{\text{extended}} = \frac{v_0}{V\left(\frac{D}{2}\right)} = 2\,\frac{v_0}{V(D)}\,. \tag{36}$$

A similar transformation has to be done on C. A certain value of $C\,(D/a)$ of the simple periodic structure corresponds to a value of

$$C\left(\frac{L}{a}\right)_{\text{extended}} = C\left(\frac{D}{2a}\right) = \frac{1}{4}\,C\left(\frac{D}{a}\right). \tag{37}$$

Since f/L is nearly proportional to C^{-1} for small values of C it is convenient to compare the values of

$$C\left(\frac{D}{a}\right)\cdot\frac{f}{D} = 2\left[C\left(\frac{L}{a}\right)\frac{f}{L}\right]_{\text{extended}}.$$

This comparison is shown in Fig. 16. For the same values of $T_h - T_c$ and v_0, the extended structure has the longer focal length because its active hot (or cold) tube is only half as long as that of the simple structure. The curve of Fig. 16 for the extended structure is not very

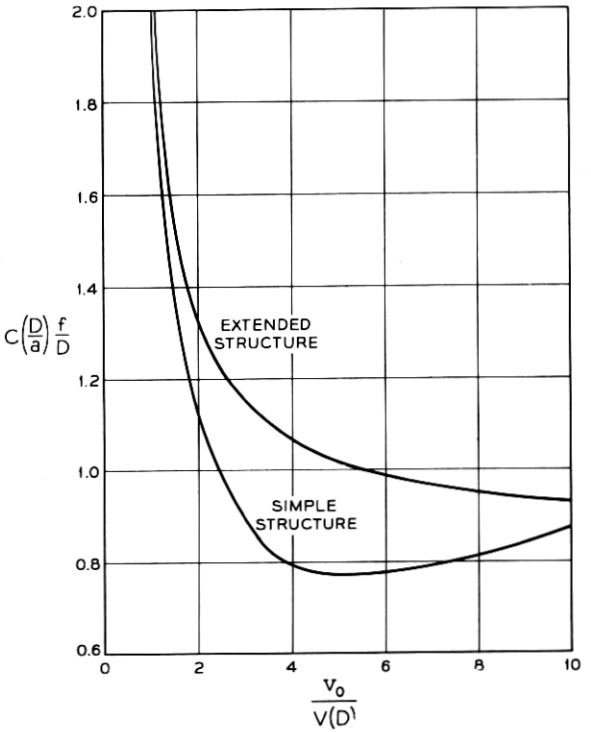

Fig. 16 — Comparison between the focal lengths of positive lenses of the simple and extended periodic structures as functions of the same normalized gas velocity $v_0/V(D)$.

accurate for values of $v_0/V(D) > 5$ because the value of $v_0/V(D) = 10$ corresponds to $v_0/V(L) = 20$ for the extended structure. For such a large value of the normalized flow velocity, our assumption of a constant input temperature to the hot (or cold) tube is incorrect.

To be able to compare the efficiencies of the two systems we need to know the power consumption of one positive lens of either of them assuming that it requires no additional power expenditure to keep the cold tubes at the temperature T_c.

This power consumption is given by

$$P = 2\pi\rho c_p a^2 \int_0^1 \{[T(x,u)]_{z=L} - [T(x,u)]_{z=0}\} x v(x)\, dx \qquad (38)$$

$v(x)$ is the gas velocity as a function of x. For viscous, laminar flow

$$v(x) = v_0(1 - x^2). \qquad (39)$$

Using (19) and (24), we obtain for the power consumption per hot tube of the simple periodic structure

$$\frac{2P_s}{\pi k D(T_h - T_c)} = \frac{v_0}{V(D)} \left\{ 1 - \frac{16R'(1)}{\beta_0^3 \left(\frac{\partial R_0}{\partial \beta}\right)_{x=1} (1 + \exp(\beta_0^2/W))} \right\} \qquad (40)$$

and with the help of (29) for the corresponding power consumption in the structure composed of extended tubes (assuming that the first term in the series of (29) describes the temperature distribution at $z = L$ sufficiently well), we obtain

$$\frac{2P_{\text{ext}}}{\pi k D(T_h - T_c)} = \frac{v_0}{V(D)} \frac{T_h - T_{ih}}{T_h - T_c} \left\{ 1 - \frac{8R_0'(1)}{\beta_0^3 \left(\frac{\partial R_0}{\partial \beta}\right)_{x=1}} \exp(-\beta_0^2/W) \right\}. \qquad (41)$$

The expression $(T_h - T_{ih})/(T_h - T_c)$ has to be substituted from (35a). The quantities represented by (40) and (41) are plotted in Fig. 17 as functions of $v_0/V(D)$. The positive lenses of the extended structure consume less power than those of the simple structure for equal amounts of gas flowing through them. This is not surprising considering that the hot tubes of the extended structure are only half as long as those of the simple structure.

To compare the two structures we require that their lenses have equal focal length which we achieve by adjusting the temperature difference between the hot and cold tubes. We then plot the ratio of the resulting power consumptions. This plot is shown in Fig. 18. The extended structure requires less power than the simple one and this ratio improves as

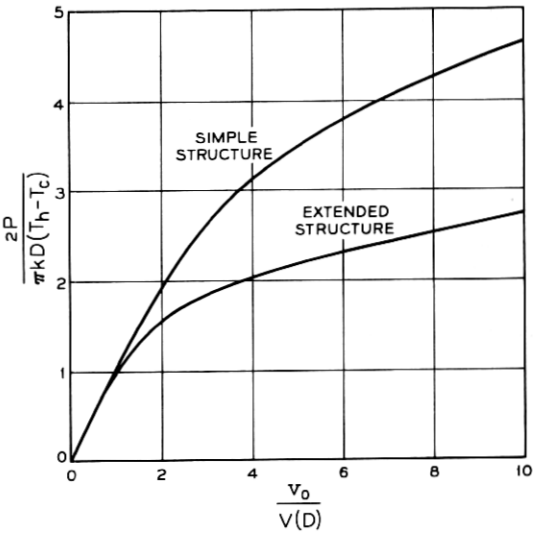

Fig. 17 — Comparison between the power consumptions of the positive lenses of the simple and extended periodic structures as functions of the same normalized gas velocities $v_0/V(D)$.

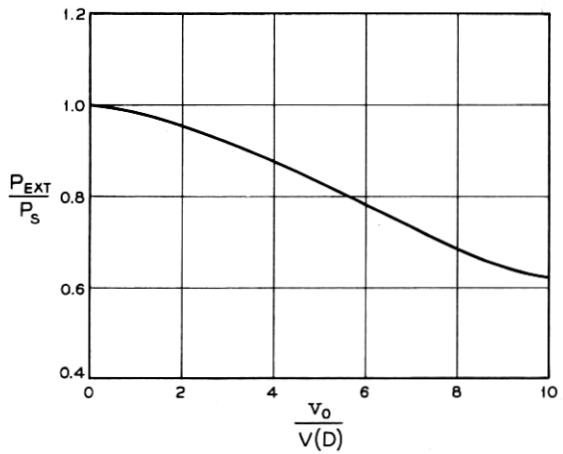

Fig. 18 — The ratio of the power consumption of the positive lenses of the extended periodic structure over the power consumption of the positive lenses of the simple periodic structure for equal focal length as a function of normalized gas velocity $v_0/V(D)$.

the flow velocity increases. It should be remembered, however, that the focal length of the extended structure (Fig. 16) is inaccurately represented for values $v_0/V(D) > 5$. This inaccuracy carries over to Fig. 18. Nevertheless, it is clear that the efficiency of the extended structure is more than 20 per cent higher than that of the simple structure for $v_0/V(D) > 6$. The additional focusing which the insulating tube sections provide pays off to some extent to make the extended structure more efficient. The improvement is not as large, however, as one might have hoped and it may be considerably poorer if the insulating tubes have the finite heat conductivity of a real material.

VI. ACKNOWLEDGMENT

The author gratefully acknowledges the help of Mrs. C. L. Beattie who wrote the machine programs for the calculation of the R- and U-functions and for part of the ray tracing.

APPENDIX

The functions to be discussed in the appendix are solutions of the differential equation

$$\frac{d^2F}{dx^2} + \frac{1}{x}\frac{dF}{dx} + k^2(1 - x^2)F = 0. \tag{42}$$

The solutions of (42) are related to Whittaker's functions $W_{\kappa,\mu}$ by

$$F = \frac{1}{x} W_{(k/4),0}(kx^2).$$

The differential equation (42) stems from an approximate formulation of a heat transfer problem.[7] Assume that a gas at a different temperature is blown into a tube with a circular cross section. The gas is supposed to flow as a viscous fluid in laminar flow with a velocity profile

$$v(r) = v_0\left(1 - \frac{r^2}{a^2}\right) \tag{43}$$

r = distance from tube axis
a = tube radius.

The stationary state of the temperature distribution T is obtained from

$$\alpha\nabla^2 T = \mathbf{v}\cdot\boldsymbol{\nabla}T \tag{44}$$

with α being a constant which contains the heat conductivity, density

and specific heat at constant pressure — all of which are assumed to be temperature independent which, strictly speaking, is not true.

The velocity has only a longitudinal component v_z given by (43). In polar coordinates r, φ, z taking $\partial/\partial\varphi = 0$ (44) can be written

$$\alpha\left\{\frac{\partial^2 T}{\partial r^2} + \frac{1}{r}\frac{\partial T}{\partial r} + \frac{\partial^2 T}{\partial z^2}\right\} = v_0\left(1 - \frac{r^2}{a^2}\right)\frac{\partial T}{\partial z}. \tag{45}$$

It is often permissible to neglect $\partial^2 T/\partial z^2$ compared to the term on the right hand side of (45). Taking

$$r = ax \tag{46}$$

and

$$T(r,z) = F(x)\exp(-\lambda z) \tag{47}$$

we get from (45)

$$\frac{d^2F}{dx^2} + \frac{1}{x}\frac{dF}{dx} + \frac{a^2 v_0 \lambda}{\alpha}(1 - x^2)F = 0. \tag{48}$$

Finally, taking

$$\lambda = k^2\frac{\alpha}{a^2 v_0} \tag{49}$$

we recognize that (48) is identical to (42).

We are interested in two types of heat transfer problems:

(1.) The tube through which the gas flows may be kept at a constant temperature T_w. We then have the boundary condition $T(a,z) = T_w$. It is more convenient to introduce a new variable

$$\theta(r,z) = T_w - T(r,z). \tag{50}$$

We can replace T by θ without changing any of equations (44) through (47). However, the boundary condition now becomes simply

$$\theta(a,z) = 0. \tag{51}$$

The functions satisfying this boundary condition are designated by

$$F(x) = R(x) \tag{52}$$

and (51) becomes

$$R(1) = 0. \tag{53}$$

The R functions have been studied in some detail.[7,8]

(2.) The second type of problem involves a tube which is a perfect

heat insulator. That means that no heat flows into or out of the walls. This assumption requires that

$$\left(\frac{\partial T}{\partial r}\right)_{r=a} = 0. \tag{54}$$

A second class of functions is obtained by setting $F(x) = U(x)$. The U-functions satisfy the same differential equation but are defined by the boundary condition

$$\left(\frac{dU}{dx}\right)_{x=1} = 0. \tag{55}$$

For convenience, both functions are normalized so that

$$R(0) = U(0) = 1. \tag{56}$$

The U-functions have not been studied to the knowledge of the author.

For series expansions of arbitrary heat distributions in terms of either the R or the U functions we need their orthogonality relations and any numerical evaluation of heat transfer problems requires the knowledge of the eigenvalues and numerical values of these functions.

The eigenvalues belonging to the R functions $R_n(x)$ will be designated as

$$k_n = \beta_n \tag{57}$$

and those of $U_n(x)$ will be designated by

$$k_n = \gamma_n . \tag{58}$$

Orthogonality Relations

Let F_n with eigenvalue k_n designate either an R_n or a U_n function. We proceed to show that

$$\int_0^1 x(1 - x^2)F_n(x)F_m(x)\,dx = 0 \qquad \text{for } n \neq m. \tag{59}$$

We have

$$F_n'' + \frac{1}{x}F_n' + k_n^2(1 - x^2)F_n = 0 \tag{60}$$

and

$$F_m'' + \frac{1}{x}F_m' + k_m^2(1 - x^2)F_m = 0. \tag{61}$$

We multiply (60) by xF_m and (61) by xF_n, subtract and integrate:

$$(k_n^2 - k_m^2) \int_0^1 x(1 - x^2)F_n(x)F_m(x)\,dx$$

$$= -\int_0^1 x\left\{\left(F_m\left(F_n'' + \frac{1}{x}F_n'\right)\right) - F_n\left(F_m'' + \frac{1}{x}F_m'\right)\right\}dx.$$

We perform partial integrations and obtain for the right hand side of this equation

$$-[xF_mF_n' - xF_nF_m']_0^1 + \int_0^1 \{F_mF_n' - F_nF_m' + x(F_m'F_n' - F_n'F_m')$$

$$- (F_mF_n' - F_nF_m')\}\,dx = (F_mF_n' - F_nF_m')_{x=1} = 0.$$

The last part of the equation follows from the boundary condition (53) or (55), depending whether F stands for an R or a U function. This calculation proves (59).

Next, we calculate the value of (59) in the case $n = m$.

$$\int_0^1 x(1 - x^2)[F_n(x)]^2\,dx = \lim_{k_m \to k_n}\left(\frac{F_mF_n' - F_nF_m'}{k_n^2 - k_m^2}\right)_{x=1}$$

$$= \left(\frac{\dfrac{\partial F_n}{\partial k}F_n' - F_n\dfrac{\partial}{\partial k}F_n'}{2k_n}\right)_{\substack{x=1\\k=k_n}}.$$

For $F_n = R_n$ we get

$$\int_0^1 x(1 - x^2)[R_n(x)]^2\,dx = \frac{1}{2\beta_n}\left[\frac{\partial R}{\partial \beta}R_n'\right]_{\substack{x=1\\\beta=\beta_b}} \tag{62}$$

and for $F_n = U_n$

$$\int_0^1 x(1 - x^2)[U_n(x)]^2\,dx = -\frac{1}{2\gamma_n}\left[U_n\frac{\partial}{\partial \gamma}U_n'\right]_{\substack{x=1\\\gamma=\gamma_n}}. \tag{63}$$

Finally, we need to determine the value of the integral over the products R_nU_m:

$$R_n'' + \frac{1}{x}R_n' + \beta_n^2(1 - x^2)R_n = 0 \tag{64}$$

$$U_m'' + \frac{1}{x}U_m' + \gamma_n^2(1 - x^2)U_m = 0, \tag{65}$$

$$(\beta_n^2 - \gamma_m^2) \int_0^1 x(1 - x^2) R_n(x) U_m(x) dx$$

$$= \int_0^1 \{x(R_n U_m'' - U_m R_n'') + R_n U_m' - U_m R_n'\} dx$$

$$= [R_n U_m' - U_m R_n']_{x=1}$$

or using (53) and (55),

$$\int_0^1 x(1 - x^2) R_n(x) U_m(x) dx = \frac{1}{\gamma_m^2 - \beta_n^2} [U_m R_n']_{x=1} . \qquad (66)$$

Calculation of the R and U Functions and Their Eigenvalues

We make the series expansion

$$F(x) = \sum_{v=0}^{\infty} C_{2v} x^{2v}. \qquad (67)$$

For the problem of interest to us $F(x)$ has to be an even function of x, for that reason only even powers of x appear in (67). The normalization

$$F(0) = 1$$

requires that (68)

$$C_0 = 1.$$

The substitution of (67) into (42), using (68), leads to

$$C_2 = -\tfrac{1}{4} k^2$$

and

$$C_{2v} = \frac{k^2}{(2v)^2} \{C_{2v-4} - C_{2v-2}\} \qquad \text{for } v \geqq 2. \qquad (69)$$

The parameter k has to be chosen so that either $F(1) = 0$ or $F'(1) = 0$ results, depending whether k and F shall represent β and R or γ and U respectively.

The fact that k^2 enters all coefficients C_{2v} makes the determination of β_n and γ_n very tedious.

A further difficulty results from the fact that the coefficients C_{2v} grow to very large values particularly for the larger values of β_n and γ_n before they decrease again. The series (67) does not converge readily for values of x close to 1. In fact, it proved impossible to compute more than the first eight R and U functions from (67) on the IBM 7094 com-

puter even using double precision since the absolute value of R and U remains between zero and one but the coefficients C_{2v} grow to values above 10^{20}. The series (67) can be used to compute R_n and U_n for x in the range $0 \leqq x \leqq 0.5$ since the powers of x decrease rapidly enough to keep the value of the product $C_{2v}\, x^{2v}$ within manageable proportions.

However, in order to cover the whole range $0 \leqq x \leqq 1$ it proved necessary to use the following series expansion:

$$F(x) = \sum_{v=0}^{\infty} D_v y^v \quad \text{with} \quad y = 1 - x \tag{70}$$

to calculate R and U in the range $0.5 \leqq x \leqq 1$.

Equation (42) expressed in terms of y reads

$$(1 - y)\frac{d^2F}{dy^2} - \frac{dF}{dy} + k^2(2y - 3y^2 + y^3)F = 0. \tag{71}$$

The coefficients D_0 and D_1 have to be properly chosen to satisfy the boundary conditions at $x = 1$. For $F = R$ we require $R(1) = 0$ so that

$$D_0 = 0$$

results. For $F = U$ we require $U'(1) = 0$ so that

$$D_1 = 0$$

results.

The substitution of (70) into (71) yields

$$\begin{aligned} &D_2 = \tfrac{1}{2}D_1\,, \qquad D_3 = \tfrac{1}{3}D_1 - \tfrac{1}{3}k^2D_0\,, \qquad D_4 = (\tfrac{1}{4} - \tfrac{1}{6}k^2)D_1 \\ &D_v = \frac{1}{v(v-1)}\{(v-1)^2 D_{v-1} - k^2(2D_{v-3} - 3D_{v-4} + D_{v-5})\}. \end{aligned} \tag{72}$$

The eigenvalue $k = \beta$ or $k = \gamma$ and the coefficient D_1 or D_0 must be chosen so that F as well as F' are continuous at $x = 0.5$ where both series expansions should coincide.

By breaking the range of x into two parts and using different series expansions to cover both parts of the range it was possible to compute the function and their eigenvalues. Table I shows the eigenvalues β_n and γ_n as well as the values of $\partial R_n/\partial\beta$, $-D_1 = R_n'$. $(\partial/\partial\gamma)U_n'$ and $D_0 = U_n$ all taken at $x = 1$. These values are needed to evaluate the integrals (62), (63) and (66).

The values of $\partial R_n/\partial\beta$ and $\partial U_n'/\partial\gamma$ were obtained from differentiation of the series (67) and evaluating it at $x = 1$. The terms of the differ-

entiated series grow very large so that only the first eight values of $\partial R/\partial\beta$ and the first six values of $\partial U'/\partial\gamma$ could be obtained. The remaining values of $\partial R/\partial\beta$ were calculated from the approximation[8]

$$\left(\frac{\partial R}{\partial \beta}\right)_{\substack{x=1\\ \beta=\beta_n}} = (-1)^n \frac{\pi}{6^{2/3}\,\Gamma\left(\frac{2}{3}\right)\beta_n^{1/3}} \tag{73}$$

which is in good agreement with the values obtained by machine calculation for larger values of n. An approximation of $\partial U/\partial\gamma$ can be obtained by using approximations similar to the ones used for the R functions in Ref. 8. One gets

$$\left(\frac{\partial U'}{\partial \gamma}\right)_{\substack{x=1\\ \gamma=\gamma_n}} = -(-1)^n \frac{\pi\gamma^{\frac{1}{3}}}{6^{\frac{1}{3}}\Gamma\left(\frac{1}{3}\right)}\,. \tag{74}$$

However, this approximation is not very good for $n \leqq 15$ so that we used the equation

$$\left(\frac{\partial U'}{\partial \gamma}\right)_{\substack{x=1\\ \gamma=\gamma_n}} = -(-1)^n \frac{\pi\gamma^{\frac{1}{3}}}{6^{\frac{1}{3}}\Gamma\left(\frac{1}{3}\right)} + \sum_{\mu=1}^{6} \frac{A_\mu}{\gamma^\mu}\,. \tag{75}$$

The coefficients A_μ were determined from the first six values of $\partial U'/\partial\gamma$ which were obtained from a machine calculation. Their values are given at the bottom of Table I.

TABLE I

n	β_n	$R_n'(1)$	$\left(\frac{\partial R(1)}{\partial\beta}\right)_{\beta=\beta_n}$	γ_n	$U_n(1)$	$\left(\frac{\partial U'(1)}{\partial\gamma}\right)_{\gamma=\gamma_n}$
0	2.70436	−1.01430	−0.50090	0	1	
1	6.67903	1.34924	0.37146	5.06750	−0.492517	0.97816
2	10.67338	−1.57232	−0.31826	9.15760	0.395509	−1.24720
3	14.6711	1.74600	0.28648	13.1972	−0.345874	1.43522
4	18.6699	−1.89090	−0.26449	17.2202	0.314047	−1.58486
5	22.6691	2.01647	0.24799	21.2355	−0.291252	1.71127
6	26.6686	−2.12814	−0.23491	25.2465	0.273806	−1.82164
7	30.6682	2.22038	0.22485	29.2549	−0.259853	1.92042
8	34.6679	−2.32214	−0.21548	33.2615	0.248332	−2.01037
9	38.6676	2.40274	0.20779	37.2669	−0.238591	2.09330
10	42.6667	−2.48992	−0.20108	41.2714	0.230199	−2.17045
11	46.6667	2.56223	0.19516	45.2752	−0.222863	2.24275
12	50.6667	−2.64962	−0.18988	49.2785	0.216371	−2.31088
13	54.6667	2.70216	0.18513	53.2813	−0.210569	2.37539
14	58.6667	−2.76421	−0.18083	57.2837	0.205216	−2.43671

$A_1 = -4.881355$ $\quad A_4 = 2.838701\ 10^4$
$A_2 = 1.536461\ 10^2$ $\quad A_5 = -1.420240\ 10^5$
$A_3 = -2.838383\ 10^3$ $\quad A_6 = 2.728875\ 10^5$

An approximate formula for β is[8]

$$\beta_n = 4n + \tfrac{8}{3}. \tag{76}$$

The β values of Table I for $n \geqq 11$ have been computed from (76).

The lowest order U function is a constant

$$U_0 = 1 \quad \text{with} \quad \gamma_0 = 0. \tag{77}$$

The γ values should converge to

$$\gamma_n = 4n + \tfrac{4}{3}. \tag{78}$$

This expression can be derived by methods analogous to those used in Ref. 8. For unknown reasons this approximation is much poorer than that for β_n. However, it appears from the values of Table I that γ_n will converge to (78) for very high values of n.

REFERENCES

1. Goubau, G., and Schwering, F., On the Guided Propagation of Electromagnetic Wave Beams, IRE Trans. *AP-9*, May, 1961, pp. 248–256.
2. Berreman, D. W., A Lens or Light Guide Using Convectively Distorted Thermal Gradients in Gases, B.S.T.J., *43*, July, 1964, pp. 1469–1475.
3. Marcuse, D., and Miller, S. E., Analysis of a Tubular Gas Lens, B.S.T.J. *43*, July, 1964, pp. 1759–1782.
4. Marcuse, D., Theory of a Thermal Gradient Gas Lens. Paper delivered at the 1965 IEEE-G-MTT Symposium, to be published in the IEEE Trans-G-MTT, Nov., 1965.
5. Miller, S. E., Alternating-Gradient Focusing and Related Properties of Convergent Lens Focusing, B.S.T.J., *43*, July, 1964, pp. 1741–1758.
6. Born, M., and Wolff, E., *Principles of Optics*, Pergamon Press, New York, 1959, p. 121 (Equation (2)).
7. Jakob, M., *Heat Transfer, 1*, John Wiley, New York, 1949, pp. 451–464.
8. Sellers, J. R., Tribus, M., and Klein, J. S., Heat Transfer to Laminar Flow in a Round Tube or Flat Conduit — The Graetz Problem Extended, Trans. Am. Soc. Mec. Eng., *78*, 1956, pp. 441–448.